LETTERS

Ligand-specific regulation of the extracellular surface of a G-protein-coupled receptor

Michael P. Bokoch[1], Yaozhong Zou[1], Søren G. F. Rasmussen[1], Corey W. Liu[2], Rie Nygaard[1], Daniel M. Rosenbaum[1], Juan José Fung[1], Hee-Jung Choi[1,3], Foon Sun Thian[1], Tong Sun Kobilka[1], Joseph D. Puglisi[2,3], William I. Weis[1,3], Leonardo Pardo[4], R. Scott Prosser[5], Luciano Mueller[6] & Brian K. Kobilka[1]

G-protein-coupled receptors (GPCRs) are seven-transmembrane proteins that mediate most cellular responses to hormones and neurotransmitters. They are the largest group of therapeutic targets for a broad spectrum of diseases. Recent crystal structures of GPCRs[1–5] have revealed structural conservation extending from the orthosteric ligand-binding site in the transmembrane core to the cytoplasmic G-protein-coupling domains. In contrast, the extracellular surface (ECS) of GPCRs is remarkably diverse and is therefore an ideal target for the discovery of subtype-selective drugs. However, little is known about the functional role of the ECS in receptor activation, or about conformational coupling of this surface to the native ligand-binding pocket. Here we use NMR spectroscopy to investigate ligand-specific conformational changes around a central structural feature in the ECS of the β_2 adrenergic receptor: a salt bridge linking extracellular loops 2 and 3. Small-molecule drugs that bind within the transmembrane core and exhibit different efficacies towards G-protein activation (agonist, neutral antagonist and inverse agonist) also stabilize distinct conformations of the ECS. We thereby demonstrate conformational coupling between the ECS and the orthosteric binding site, showing that drugs targeting this diverse surface could function as allosteric modulators with high subtype selectivity. Moreover, these studies provide a new insight into the dynamic behaviour of GPCRs not addressable by static, inactive-state crystal structures.

In the ligand-free basal state, GPCRs exist in an equilibrium of conformations[6]. Ligand binding modulates receptor function by stabilizing different intramolecular interactions and establishing a new conformational equilibrium. Activating ligands (agonists) stabilize receptor conformations that increase signalling through G proteins; inhibiting ligands (inverse agonists) stabilize other conformations that decrease the basal, agonist-independent level of signalling (Supplementary Fig. 1). When a GPCR is activated, structural changes occur in the cytoplasmic G-protein-coupling domains. These changes have been characterized for several receptors, including rhodopsin[7–10] and the β_2 adrenergic receptor (β_2AR)[11–13]. Recent solid-state NMR data show that light activation of rhodopsin also induces conformational changes in extracellular loop (ECL) 2 (ref. 14). In rhodopsin, ECL2 forms a structured cap over the covalently bound ligand retinal and interacts with transmembrane (TM) segments involved in activation. However, little is known about the effects of diffusible ligand binding on the extracellular domains of other family A GPCRs, in which ECL2 is displaced away from the ligand-binding pocket. Here we show that ligands known to affect cytoplasmic domain conformation differentially also stabilize distinct ECS conformations (Supplementary Fig. 1).

Understanding conformational changes in the ECS of GPCRs may provide new avenues for drug design. Comparison of the crystallographically identified orthosteric binding pockets of β_2AR and β_1AR reveals that 15 of 16 amino acids (94%) are identical[1,5]. This observation underscores the challenge of identifying subtype-selective drugs for families containing several closely related receptors (for example adrenergic, serotonin or dopamine receptors)[15]. In contrast, although the backbone structure of the β_2AR and β_1AR extracellular domains are similar, 22 of 39 residues (56%) in ECLs 2 and 3 differ. The ECS therefore provides a diverse site for the development of subtype-selective drugs.

Most of the β_2AR ECS consists of ECL2, connecting TMs 4 and 5, and ECL3, connecting TMs 6 and 7 (Fig. 1a)[1,2]. ECL2 forms a two-turn α-helix that is displaced away from the ligand-binding site entrance (Fig. 1b). Two disulphide bonds stabilize ECL2, one within the loop and one to the end of TM3. A salt bridge formed by Lys $305^{7.32}$ and Asp 192^{ECL2} connects ECL3–TM7 to ECL2 (superscripts in this form indicate Ballesteros–Weinstein numbering for conserved GPCR residues)[16]. Carazolol is an inverse agonist that binds in the orthosteric pocket formed by TMs 3, 5, 6 and 7. The only direct interaction between the ECS and carazolol is through an aromatic interaction with Phe 193^{ECL2}. Given these specific associations between ECLs, the orthosteric ligand-binding site and TMs involved in activation[17], we speculated that β_2AR extracellular domains and the associated salt bridge rearrange on activation.

To monitor the environment around the Lys 305–Asp 192 salt bridge by NMR, we selectively labelled lysine side chains in a modified β_2AR (β_2AR365) with carbon-13 by reductive methylation[18] (Methods, Supplementary Figs 2–4 and Supplementary Table 1):

$$\text{R-}\ddot{\text{N}}\text{H}_2 \rightleftharpoons \text{R-}\overset{+}{\text{N}}\text{H}_3 \xrightarrow[\text{NaBH}_3\text{CN}]{^{13}\text{CH}_2\text{O}} \text{R-}\ddot{\text{N}}(^{13}\text{CH}_3)_2 \rightleftharpoons \text{R-}\overset{+}{\text{N}}\text{H}(^{13}\text{CH}_3)_2 \quad (1)$$

This approach exploits the sensitivity of methyl groups as NMR probes for the analysis of large protein structure and dynamics[19]. Reductive methylation adds two [^{13}C]methyl groups to the ε-NH_2 of lysine side chains and the α-NH_2 at the receptor amino terminus. The [^{13}C]dimethyllysines serve as conformational probes in two-dimensional ^{1}H–^{13}C correlation NMR experiments. Dimethylation does not alter the positive charge on the lysine residue (equation (1)) and causes little structural perturbation[20]. We observed no significant changes between the crystal structure of a methylated β_2AR–Fab complex bound to carazolol and that of the non-methylated receptor (Supplementary Fig. 5 and Supplementary Table 2). Reductively [^{13}C]methylated β_2AR ([^{13}C]methyl-β_2AR) has ligand-binding properties identical to those of unlabelled β_2AR, and G-protein coupling is unimpaired (Supplementary Fig. 6).

[1]Department of Molecular and Cellular Physiology, [2]Stanford Magnetic Resonance Laboratory, and [3]Department of Structural Biology, Stanford University School of Medicine, Stanford, California 94305, USA. [4]Laboratori de Medicina Computacional, Unitat de Bioestadística, Universitat Autònoma de Barcelona, 08193 Bellaterra (Barcelona), Spain. [5]Department of Chemistry, University of Toronto, UTM, Mississauga, Ontario, Canada L5L 1C6. [6]Bristol-Myers Squibb Pharmaceutical Research Institute, Princeton, New Jersey 08543, USA.

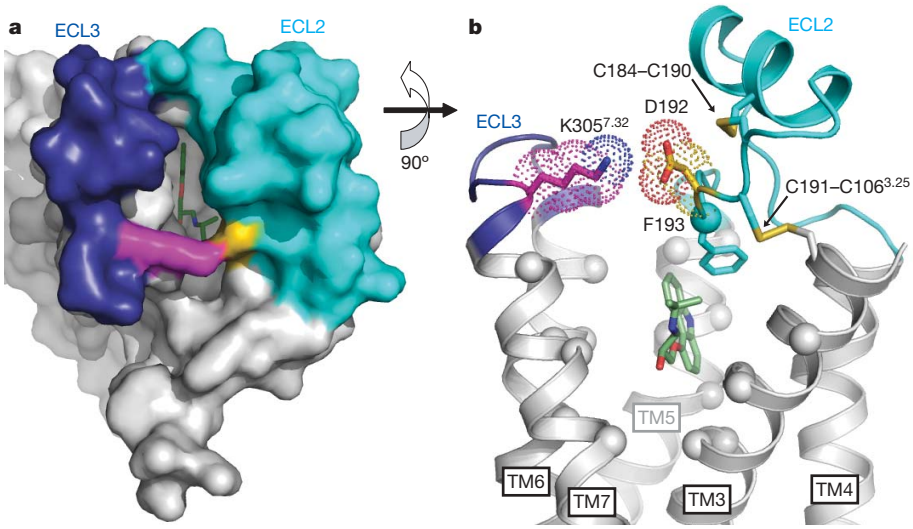

Figure 1 | Extracellular domains of carazolol-bound β_2AR. a, The extracellular surface (ECS) of β_2AR showing ECL2 (cyan, Met 171–Ala 198), ECL3 (dark blue, His 296–Glu 306), Lys 305$^{7.32}$ (magenta), Asp 192 (yellow) and the inverse agonist carazolol (green). ECL1 (Met 96–Phe 108) is part of the ECS but is not coloured. **b**, Intramolecular and ligand-binding interactions. Spheres indicate the α carbons of residues in direct contact with carazolol (at least one atom within 4 Å distance). Disulphide bonds are shown as yellow sticks. Other colours are the same as in **a**. Transmembrane helices 1 and 2 have been removed for clarity. Asp 192 and Lys 305 form the only lysine salt bridge observed in the crystal structure. The relative accessibilities of Asp 192 and Lys 305 are 35% and 75%, respectively, compared with the accessibility of that residue type in an extended Ala-x-Ala tripeptide[30].

Intense peaks from dimethylamines (dimethyllysines and the dimethyl-amino terminus) are observed in the ^{1}H–^{13}C NMR spectrum of [^{13}C]methyl-β_2AR bound to the inverse agonist carazolol in detergent buffer (Fig. 2, dimethylamine region; Supplementary Fig. 7, full spectral width). We used both heteronuclear single-quantum coherence (HSQC) and saturation transfer differencing (STD)-filtered ^{1}H-detected heteronuclear multiple-quantum coherence (HMQC) pulse sequences throughout this work; STD-filtered HMQC improved the spectral quality at the expense of longer acquisition times (Supplementary Fig. 8).

Several features of the [^{13}C]methyl-β_2AR NMR spectrum are notable (Fig. 2a). The sharpest peak is assigned to the dimethyl-amino terminus on the basis of protease digestion (Fig. 2b and Supplementary Fig. 9). The remaining peaks are assigned to dimethyllysines. The region is dominated by a cluster of overlapping peaks (centred at ^{1}H chemical shift 2.8 p.p.m.) attributed to solvent-exposed, highly mobile lysines. The intensity of this cluster is decreased by about 50% after the mutation of seven cytoplasmic lysines to arginine (Fig. 2b and Supplementary Fig. 10). Two broad dimethyllysine peaks are shifted upfield in the ^{1}H dimension (Fig. 2a, peaks 1 and 2). These peaks represent the two [^{13}C]methyl groups on Lys 305, as determined by mutation of Lys 305 to Arg (Fig. 2c and Supplementary Fig. 10). The fine structure features in peaks 1 and 2 might suggest conformational heterogeneity; however, they are most probably due to relatively low signal-to-noise ratios and subtle baseline distortions.

Lys 305 is the only lysine that forms a salt bridge in the β_2AR crystal structure, which is consistent with the unique chemical shifts of peaks 1 and 2. The presence of two peaks implies that the two methyl groups on Lys 305 exist in non-equivalent chemical environments[21–23]. The two peaks merge under conditions of increased temperature and ionic strength, presumably as a result of weakening of the salt bridge (Supplementary Fig. 11). Reduction of the disulphide bonds stabilizing ECL2 in the β_2AR abolishes the Lys 305 peaks (Supplementary Fig. 12), demonstrating that the salt bridge is sensitive to conformational changes in the ECS. Taken as a whole, these data show that the Lys 305–Asp 192 salt bridge is formed in solution as well as in crystal lattices for carazolol-bound β_2AR[2,24]. This conclusion is further supported by measurements of ^{13}C transverse relaxation (T_2) times indicating restricted motion of Lys 305 compared with other β_2AR lysines (Supplementary Fig. 13 and Supplementary Table 3).

The Lys 305 peaks are a probe for conformational changes in the receptor ECS. Both peaks are present in the NMR spectrum of unliganded β_2AR, indicating that the Lys 305–Asp 192 salt bridge also forms in the basal state (Fig. 3a). Two differences are seen relative to the carazolol-bound state (Fig. 3b). First, peaks 1 and 2 have a larger upfield shift in the ^{1}H dimension. Second, the ^{13}C chemical-shift separation between peaks 1 and 2 is increased. These data show that carazolol binding alters the chemical environment around Lys 305, demonstrating a change in the ECS. In contrast with inverse agonists, neutral antagonists (for example alprenolol) do not alter basal receptor activity. As might be predicted on the basis of ligand efficacy, NMR detects no difference in Lys 305 chemical shifts between unliganded and alprenolol-bound β_2AR (Fig. 3c).

The inverse agonist-induced conformational change (Fig. 3) probably involves Phe 193 in ECL2 (Fig. 1b), which forms a favourable edge-to-face interaction with the tricyclic aromatic ring of carazolol in the β_2AR crystal structure[1]. Nearly identical interactions are observed with other inverse agonists: Phe 193 and timolol in β_2AR[24], and the homologous Phe 201 and cyanopindolol in β_1AR[5]. By contrast, alprenolol has a single aromatic ring that cannot interact strongly with Phe 193 when docked at the carazolol position. Molecular dynamics simulations show that Phe 193 adopts the *trans* conformation pointing towards TM5 in the presence of carazolol, but it has increased mobility and is able to assume multiple conformations in the alprenolol-bound state (Supplementary Fig. 14). Phe 193 can form close encounters (less than 5 Å) with the Lys 305 amine when alprenolol is bound. The observed upfield chemical shift change of peaks 1 and 2 in alprenolol-bound receptor relative to carazolol-bound receptor is therefore most probably due to aromatic ring current effects, although we cannot exclude the possibility of other changes in ECS conformation.

Agonists induce ECS conformational changes that differ from those induced by inverse agonists. Adding formoterol, a β_2AR agonist with nanomolar affinity, attenuates the Lys 305 resonances (Fig. 4a, b). The effect is titratable (Supplementary Fig. 15) and reverses when formoterol is replaced by carazolol by dialysis (Fig. 4c). Attenuation of Lys 305 resonances was also observed with another, structurally distinct high-affinity agonist (Supplementary Fig. 16). These NMR data suggest that the Lys 305–Asp 192 salt bridge is weakened in the β_2AR active state. A loss of interaction with Asp 192 would abolish the unique chemical environment of Lys 305. On the basis of the β_2AR

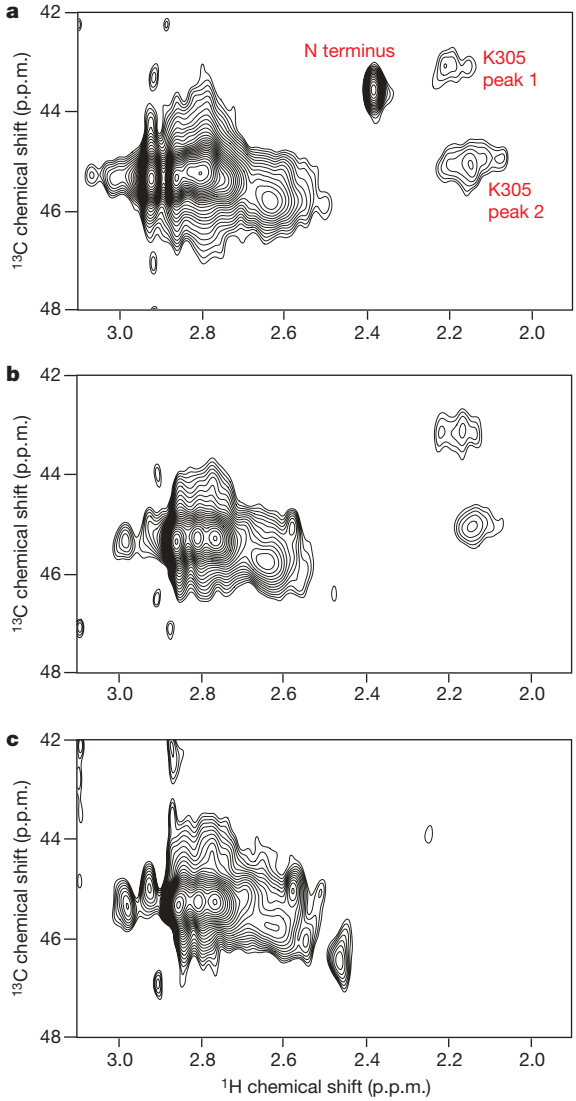

Figure 2 | Dimethyllysine NMR spectroscopy of [^{13}C]methyl-β_2AR and assignment of Lys 305. **a**, Dimethylamine region of STD-filtered ^{1}H–^{13}C HMQC spectrum of carazolol-bound β_2AR365, containing 14 Lys residues and an N-terminal Flag–TEV sequence (Supplementary Fig. 2). **b**, Spectrum of β_2AR365 with seven cytoplasmic Lys→Arg mutations (β_2AR365 Δ7Lys) and the N terminus removed by TEV proteolysis. **c**, Spectrum of β_2AR365 Δ7Lys plus the Lys 305→Arg mutation and the N terminus removed by TEV proteolysis.

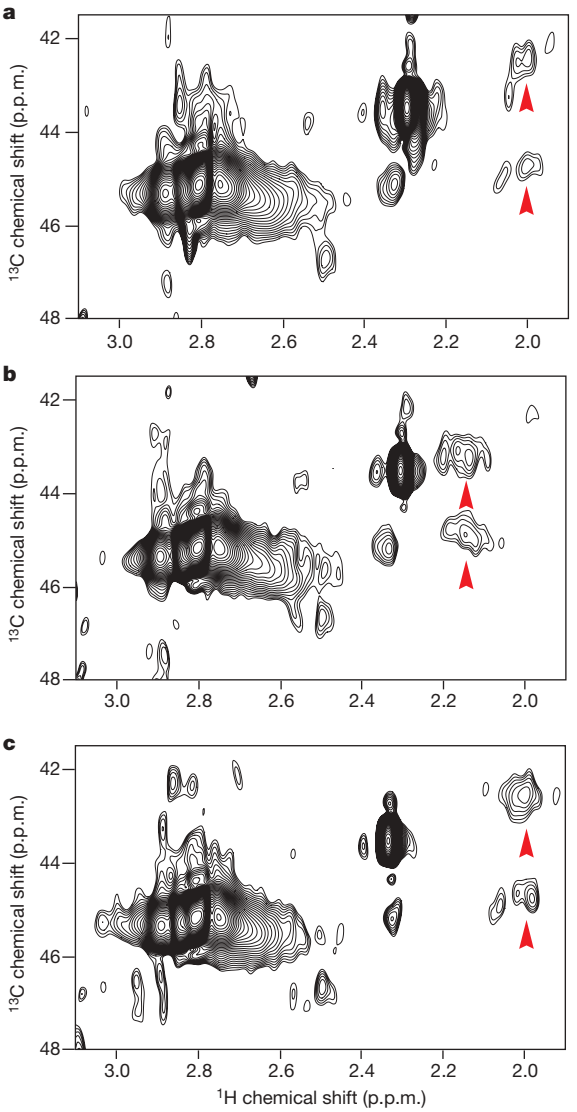

Figure 3 | Effect of inverse agonist and antagonist on the [^{13}C]dimethyl-Lys 305 NMR resonances. **a**–**c**, HSQC spectra of unliganded β_2AR (about 60 μM) (**a**), β_2AR bound to inverse agonist carazolol (**b**) and β_2AR bound to the neutral antagonist alprenolol (**c**).

crystal structure, we estimate that a distance increase of 2.9 Å between the Cα carbons of Asp 192 and Lys 305 is the minimum needed to disrupt the geometrical criteria for a salt bridge established previously[25]. At equilibrium, the fraction of Lys 305 liberated from the salt bridge would be indistinguishable from solvent-exposed lysine residues (at 2.8 p.p.m. ^{1}H chemical shift), explaining the absence of any new peaks. Alternatively, if agonists were to induce conformational fluctuations on the millisecond timescale, line broadening would attenuate the signal for Lys 305. In either case, we interpret the formoterol-induced conformational change as a relative motion between ECL3–TM7 and ECL2. Conformational changes involving ECL2 are compatible with circular dichroism experiments demonstrating agonist-induced changes in the extracellular disulphide bond linking ECL2 and TM3 in the 5-hydroxytryptamine$_{4(a)}$ receptor[26].

On the basis of our NMR results and computational modelling, we propose that the extracellular ends of TMs 6 and 7 move on activation (Fig. 4d). In brief, formoterol-activated β_2AR was modelled on the basis of the crystal structure of ligand-free opsin[9] and a relaxed conformation of the highly distorted Pro 288$^{6.50}$-induced kink (Supplementary Fig. 17).

In this active state model, an inward movement at the extracellular end of TM6 permits the known interaction between Asn 293$^{6.55}$ and the chiral β-hydroxyl of the agonist[27]. This motion, simultaneous with outward motion at the intracellular end of TM6 towards TM5 (ref. 9), agrees with the activation model derived from engineering GPCRs with metal-ion-binding sites[28,29]. The TM6 motion necessitates a lateral displacement of TM7 that reorients the Lys 305$^{7.32}$ salt bridge in agreement with NMR spectroscopy (Fig. 4). Inverse agonists may function in part by stabilizing bulky hydrophobic interactions with Phe 193^{ECL2} that block the motion of TM6.

Thus, NMR spectroscopy can be used to investigate structural changes in GPCRs, although the isotopic labelling methods employed here are limited to monitoring changes in the environment and dynamics of accessible lysine side chains. We provide direct biophysical evidence for three distinct conformations of the β_2AR extracellular surface: one for an unliganded receptor or a neutral antagonist, one for an inverse agonist, and one for an agonist (Fig. 4e). These conformations correspond to distinct functional behaviour. Unliganded and alprenolol-bound β_2AR are both able to couple to G_s, which is consistent with the basal activity of the receptor and the efficacy of alprenolol (neutral antagonist). In contrast, the inverse agonist carazolol prevents receptor–G_s coupling. Finally, agonists promote the strongest coupling. Ligands binding to the extracellular surface could therefore

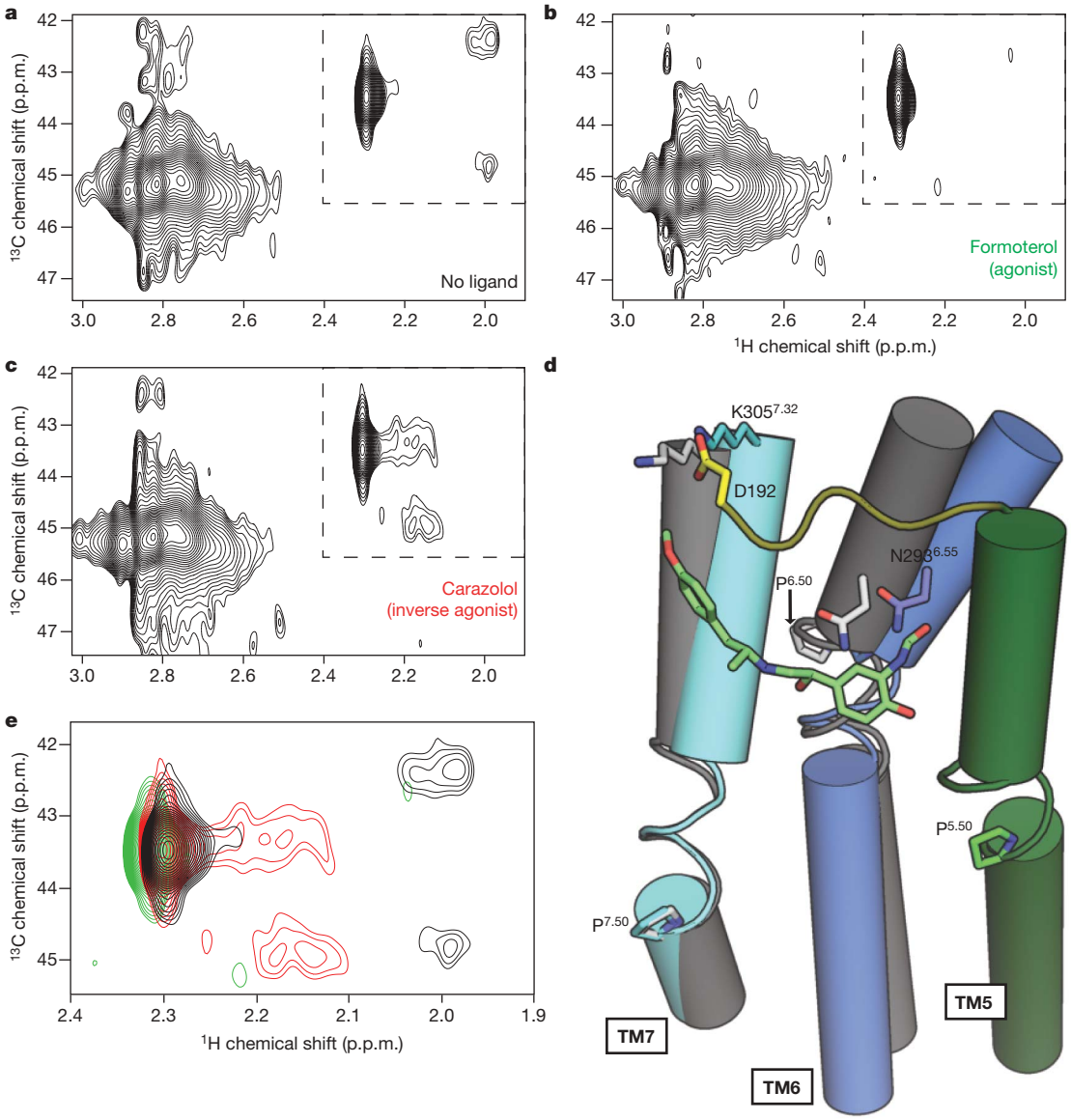

Figure 4 | Activation of β_2AR by formoterol. **a**–**c**, STD-filtered HMQC spectra of unliganded β_2AR (about 60 μM) (**a**), the same sample bound to a saturating concentration (320 μM) of agonist (*R*,*R*)-formoterol (**b**) and the same sample after replacing formoterol with the inverse agonist carazolol by dialysis (**c**). **d**, Model of β_2AR activation by formoterol (see Supplementary Fig. 16). Coloured helices, loops and side chains represent the carazolol-bound crystal structure. Grey helices and white side chains indicate the active-state model. Green sticks indicate (*R*,*R*)-formoterol and yellow indicates ECL2. **e**, Overlay of spectra corresponding to dashed regions shown in **a**–**c**. The spectrum of unliganded β_2AR from **a** is shown in black, agonist-bound β_2AR from **b** in green, and inverse agonist-bound β_2AR from **c** in red.

modulate receptor function, either by influencing the binding of orthosteric ligands or by direct allosteric modulation of cytoplasmic domain conformation (Supplementary Fig. 1). Although the specific salt bridge used to monitor these conformations may not be present in other GPCRs, it is ideally positioned to monitor ECS conformations in the β_2AR, and it is likely that our findings about ligand-induced changes in the ECS are relevant for other family A GPCRs.

METHODS SUMMARY

NMR spectroscopy of [^{13}C]methyl-β_2AR. Human β_2AR, tagged with an N-terminal Flag–tobacco etch virus (TEV) protease sequence, and truncated after residue Gly 365 (β_2AR365; Supplementary Fig. 2) was expressed in *Spodoptera frugiperda* (Sf9) insect cells with recombinant baculovirus. Sf9 cell membranes were solubilized with dodecylmaltoside and purified by sequential antibody affinity and alprenolol affinity chromatography, as described previously[3]. ^{13}C-Methyl labelling was performed by sequentially adding excess sodium cyanoborohydride followed by [^{13}C]formaldehyde to purified β_2AR. Methylation reagents were removed by extensive dialysis (unliganded β_2AR) or by anion-exchange chromatography (carazolol-bound β_2AR). For NMR spectroscopy, [^{13}C]methyl-β_2AR was dialysed against buffer containing 20 mM HEPES, pH 7.4, 100 mM NaCl and 0.1% dodecylmaltoside prepared in 98% $^{2}H_2O$ and concentrated to a final concentration of 50–200 μM. Two-dimensional ^{1}H–^{13}C correlation spectra of [^{13}C]methyl-β_2AR were recorded at 800 MHz for about 8 h (HSQC) or 24 h (STD-filtered HMQC) at 25 °C. Both pulse sequences used WATERGATE water suppression. See Supplementary Fig. 8 for all parameters and full details of NMR spectroscopy.

Crystal structure of [^{13}C]methyl-β_2AR–Fab5 complex. [^{13}C]Methyl-β_2AR–Fab5 complex was prepared and crystallized as described previously[3]. Diffraction images were obtained on a microfocus beam line, and the structure was solved by molecular replacement using β_2AR–Fab5 (PDB accession code 2R4R) as a search model.

Full Methods and any associated references are available in the online version of the paper at www.nature.com/nature.

Received 24 June; accepted 6 November 2009.

1. Rosenbaum, D. M. *et al.* GPCR engineering yields high-resolution structural insights into β_2-adrenergic receptor function. *Science* **318**, 1266–1273 (2007).

2. Cherezov, V. *et al.* High-resolution crystal structure of an engineered human β_2-adrenergic G protein-coupled receptor. *Science* **318,** 1258–1265 (2007).
3. Rasmussen, S. G. *et al.* Crystal structure of the human β_2 adrenergic G-protein-coupled receptor. *Nature* **450,** 383–387 (2007).
4. Jaakola, V. P. *et al.* The 2.6 angstrom crystal structure of a human A2A adenosine receptor bound to an antagonist. *Science* **322,** 1211–1217 (2008).
5. Warne, T. *et al.* Structure of a β_1-adrenergic G-protein-coupled receptor. *Nature* **454,** 486–491 (2008).
6. Kobilka, B. K. & Deupi, X. Conformational complexity of G-protein-coupled receptors. *Trends Pharmacol. Sci.* **28,** 397–406 (2007).
7. Farrens, D. L., Altenbach, C., Yang, K., Hubbell, W. L. & Khorana, H. G. Requirement of rigid-body motion of transmembrane helices for light activation of rhodopsin. *Science* **274,** 768–770 (1996).
8. Altenbach, C., Kusnetzow, A. K., Ernst, O. P., Hofmann, K. P. & Hubbell, W. L. High-resolution distance mapping in rhodopsin reveals the pattern of helix movement due to activation. *Proc. Natl Acad. Sci. USA* **105,** 7439–7444 (2008).
9. Park, J. H., Scheerer, P., Hofmann, K. P., Choe, H. W. & Ernst, O. P. Crystal structure of the ligand-free G-protein-coupled receptor opsin. *Nature* **454,** 183–187 (2008).
10. Scheerer, P. *et al.* Crystal structure of opsin in its G-protein-interacting conformation. *Nature* **455,** 497–502 (2008).
11. Ghanouni, P. *et al.* Functionally different agonists induce distinct conformations in the G protein coupling domain of the β_2 adrenergic receptor. *J. Biol. Chem.* **276,** 24433–24436 (2001).
12. Swaminath, G. *et al.* Probing the β_2 adrenoceptor binding site with catechol reveals differences in binding and activation by agonists and partial agonists. *J. Biol. Chem.* **280,** 22165–22171 (2005).
13. Yao, X. *et al.* Coupling ligand structure to specific conformational switches in the β_2-adrenoceptor. *Nature Chem. Biol.* **2,** 417–422 (2006).
14. Ahuja, S. *et al.* Helix movement is coupled to displacement of the second extracellular loop in rhodopsin activation. *Nature Struct. Mol. Biol.* **16,** 168–175 (2009).
15. Conn, P. J., Christopoulos, A. & Lindsley, C. W. Allosteric modulators of GPCRs: a novel approach for the treatment of CNS disorders. *Nature Rev. Drug Discov.* **8,** 41–54 (2009).
16. Ballesteros, J. A. & Weinstein, H. Integrated methods for the construction of three-dimensional models and computational probing of structure-function relations in G-protein coupled receptors. *Methods Neurosci.* **25,** 366–428 (1995).
17. Nygaard, R., Frimurer, T. M., Holst, B., Rosenkilde, M. M. & Schwartz, T. W. Ligand binding and micro-switches in 7TM receptor structures. *Trends Pharmacol. Sci.* **30,** 249–259 (2009).
18. Zhang, M. & Vogel, H. J. Determination of the side chain pK_a values of the lysine residues in calmodulin. *J. Biol. Chem.* **268,** 22420–22428 (1993).
19. Tugarinov, V., Hwang, P. M., Ollerenshaw, J. E. & Kay, L. E. Cross-correlated relaxation enhanced ^{1}H–^{13}C NMR spectroscopy of methyl groups in very high molecular weight proteins and protein complexes. *J. Am. Chem. Soc.* **125,** 10420–10428 (2003).
20. Jentoft, J. E., Jentoft, N., Gerken, T. A. & Dearborn, D. G. ^{13}C NMR studies of ribonuclease A methylated with [^{13}C]formaldehyde. *J. Biol. Chem.* **254,** 4366–4370 (1979).
21. Gerken, T. A., Jentoft, J. E., Jentoft, N. & Dearborn, D. G. Intramolecular interactions of amino groups in ^{13}C reductively methylated hen egg-white lysozyme. *J. Biol. Chem.* **257,** 2894–2900 (1982).
22. Sherry, A. D. & Teherani, J. Physical studies of ^{13}C-methylated concanavalin A. pH- and Co^{2+}-induced nuclear magnetic resonance shifts. *J. Biol. Chem.* **258,** 8663–8669 (1983).
23. Abraham, S. J., Hoheisel, S. & Gaponenko, V. Detection of protein-ligand interactions by NMR using reductive methylation of lysine residues. *J. Biomol. NMR* **42,** 143–148 (2008).
24. Hanson, M. A. *et al.* A specific cholesterol binding site is established by the 2.8 Å structure of the human β_2-adrenergic receptor. *Structure* **16,** 897–905 (2008).
25. Kumar, S. & Nussinov, R. Relationship between ion pair geometries and electrostatic strengths in proteins. *Biophys. J.* **83,** 1595–1612 (2002).
26. Baneres, J. L. *et al.* Molecular characterization of a purified 5-HT4 receptor: a structural basis for drug efficacy. *J. Biol. Chem.* **280,** 20253–20260 (2005).
27. Wieland, K., Zuurmond, H. M., Krasel, C., Ijzerman, A. P. & Lohse, M. J. Involvement of Asn-293 in stereospecific agonist recognition and in activation of the β_2-adrenergic receptor. *Proc. Natl Acad. Sci. USA* **93,** 9276–9281 (1996).
28. Elling, C. E. *et al.* Metal ion site engineering indicates a global toggle switch model for seven-transmembrane receptor activation. *J. Biol. Chem.* **281,** 17337–17346 (2006).
29. Schwartz, T. W., Frimurer, T. M., Holst, B., Rosenkilde, M. M. & Elling, C. E. Molecular mechanism of 7TM receptor activation—a global toggle switch model. *Annu. Rev. Pharmacol. Toxicol.* **46,** 481–519 (2006).
30. Hubbard, S. J., Campbell, S. F. & Thornton, J. M. Molecular recognition. Conformational analysis of limited proteolytic sites and serine proteinase protein inhibitors. *J. Mol. Biol.* **220,** 507–530 (1991).

Supplementary Information is linked to the online version of the paper at www.nature.com/nature.

Acknowledgements We acknowledge support from National Institutes of Health, grants NS028471 (B.K.K.) and GM56169 (W.I.W.), the Stanford Medical Scientist Training Program (M.P.B.), the Lundbeck Foundation (S.G.F.R.), the University of Copenhagen and 7TM Pharma (R.N.), and the Instituto de Salud Carlos III (L.P.).

Author Contributions M.P.B. designed experiments, purified, labelled and functionally characterized β_2AR, collected and analysed NMR data and wrote the paper. Y.Z. made, expressed and purified β_2AR lysine mutants and collected NMR data. S.G.F.R. expressed and purified β_2AR for NMR and crystallized the ^{13}C-methylated β_2AR–Fab complex. C.W.L. designed, optimized and supervised NMR experiments and collected NMR data. D.M.R., H.-J.C. and W.I.W. collected diffraction data and refined the structure of the ^{13}C-methylated β_2AR–Fab complex. R.N. collected and analysed NMR data and optimized data processing. J.J.F. performed G-protein-coupling assays on labelled β_2AR. F.S.T. prepared insect cell cultures and purified β_2AR. T.S.K. purified β_2AR. J.D.P. advised on NMR spectroscopy experiments. L.P. performed molecular modelling and molecular dynamics simulations. R.S.P. designed and optimized NMR experiments, wrote NMR pulse sequences and collected data. L.M. conceived of lysine methylation of the β_2AR, wrote NMR pulse sequences and designed NMR experiments. B.K.K. supervised the overall project, designed experiments, collected diffraction data and wrote the paper.

Author Information Coordinates and structure factors for [^{13}C]methyl-β_2AR–Fab5 have been deposited in the Protein Data Bank under accession code 3KJ6. Reprints and permissions information is available at www.nature.com/reprints. The authors declare no competing financial interests. Correspondence and requests for materials should be addressed to B.K.K. (kobilka@stanford.edu).

METHODS

Buffers. Buffer A is 20 mM HEPES, pH 7.4, 100 mM NaCl, 0.1% dodecylmaltoside. Buffer B is 20 mM HEPES, pH 7.4, 80 mM NaCl, 0.1% dodecylmaltoside. Buffer C is 20 mM HEPES, pH 7.4, 60 mM NaCl, 0.1% dodecylmaltoside. Buffer D is 20 mM HEPES, pH 7.4, 350 mM NaCl, 0.1% dodecylmaltoside. Buffer E is buffer A plus 2 mM $CaCl_2$ and 0.01% cholesterol hemisuccinate. Buffer F is buffer A plus 5 mM EDTA and 0.01% cholesterol hemisuccinate.

Preparation of modified β_2-adrenergic receptors for NMR. The coding sequence of wild-type human β_2AR was cloned into the pFastBac1 Sf9 insect cell expression vector (Invitrogen) and modified as described previously[3]. For small-scale expression trials (1 litre or less), recombinant baculovirus was made with the Bac-to-Bac system (Invitrogen). For large NMR and crystallography-scale expressions, the β_2AR cDNA was subcloned into the pVL1392 transfer vector and recombinant baculovirus was made with the BestBac system (Expression Systems). All cells were cultured in ESF 921 insect cell medium (Expression Systems). β_2AR365 (Supplementary Fig. 2) was expressed in Sf9 insect cells infected with baculovirus and solubilized in 1% *n*-dodecyl-β-D-maltopyranoside (dodecylmaltoside; Anatrace) in accordance with methods described previously[31]. M1 Flag affinity chromatography (Sigma) was used as the initial purification step. Flag-purified receptor was treated with 100 μM tris(2-carboxyethyl)phosphine followed by two additions of 2 mM iodoacetamide (twice, each for 1 h on ice) to alkylate reactive cysteine residues that can cause disulphide aggregation (these and all other reagents were from Sigma unless otherwise noted). Alternatively, β_2AR365 was labelled with the cysteine-reactive fluorophore monobromobimane before alkylation, to assess ligand-induced conformational changes[32]. Alkylation was quenched by the addition of 5 mM L-cysteine. Functional β_2AR365 was then selectively purified by alprenolol-Sepharose chromatography[31]. The next preparation steps varied depending on the particular NMR sample being prepared.

Preparation of carazolol-bound [^{13}C]methyl-β_2AR365. β_2AR365 (purified by alprenolol-Sepharose) was reductively methylated by sequentially adding 10 mM freshly prepared sodium cyanoborohydride, briefly vortex-mixing, and then adding 10 mM ^{13}C-enriched (99%) formaldehyde (CLM-806-1; Cambridge Isotope Labs). We feel that the order of reagent addition is important. We preferred to first set a reducing environment in solution to avoid protein cross-linking by formaldehyde. The reductive methylation reaction was then allowed to proceed overnight (minimum 8 h) at 4 °C with nutation. A second addition of sodium cyanoborohydride and [^{13}C]formaldehyde was made exactly as before, followed by another 4 h incubation at 4 °C. [^{13}C]Methyl-β_2AR365 was then dialysed extensively against buffer A plus 1 μM carazolol to remove unreacted methylation reagents and replace alprenolol with carazolol.

Reductive methylation destroys the antigenicity of the M1 Flag epitope, so we could not use a second M1 Flag affinity step to concentrate [^{13}C]methyl-β_2AR365 to NMR concentrations. The receptor was instead loaded onto Q Sepharose anion-exchange resin equilibrated in buffer B. We estimate the capacity of Q Sepharose to be about 2.5 mg of [^{13}C]methyl-β_2AR365 per ml of resin. Binding is largely mediated through the acidic Flag epitope (amino-acid sequence DYKDDDDA), because TEV-cleaved β_2AR365 does not bind tightly to Q Sepharose resin. The column was then washed with three column volumes of buffer C plus 1 μM carazolol, and eluted with buffer D plus 1 μM carazolol. A one-tenth volume of a saturated cholesterol hemisuccinate solution in buffer A was added to the eluate to enhance receptor stability. [^{13}C]methyl-β_2AR365 was typically eluted at a concentration of about 100 μM as determined by measurement of carazolol fluorescence[33]. N-linked glycosylations were removed by treatment with PNGase F (New England BioLabs; 750 units per mg of β_2AR365) for 1 h at 22–25 °C. The sample was dialysed extensively against buffer A plus 100 nM carazolol, followed by two dialysis steps against a small volume (about 25 ml) of buffer A prepared in 98% ^2H_2O (Cambridge Isotope Labs) plus 100 nM carazolol. Receptor was then concentrated to ≈200 μM with a 100-kDa cutoff Vivaspin concentrator (Vivascience). It is important to wash the concentrator membrane extensively with water, followed by ^2H_2O, to remove as much glycerol as possible because it can interfere with NMR spectroscopy.

Final NMR samples (about 270 μl) were loaded into Shigemi microtubes susceptibility-matched to ^2H_2O (Shigemi Inc.) and sealed. Carazolol-bound [^{13}C]methyl-β_2AR samples remained stable for more than four months with no visible precipitation, degradation of NMR spectral quality, or decrease in bound carazolol fluorescence. This method was used to prepare the samples shown in Fig. 2a and Supplementary Figs 7–9 and 13.

Preparation of unliganded [^{13}C]methyl-β_2AR365. β_2AR365 (purified by alprenolol-Sepharose, 2 mM $CaCl_2$ added) was loaded directly onto M1 resin for a second Flag affinity step. After loading, the column was washed at 10 ml h^{-1} with six column volumes of buffer E plus 30 μM atenolol. Atenolol is an antagonist with relatively low affinity for the β_2AR ($K_d \approx 1$ μM)[34]. This wash step was included to displace the higher-affinity antagonist alprenolol ($K_d \approx 1$ nM) from β_2AR365 by competition. The Flag M1 column was then washed extensively with buffer E to remove atenolol and guarantee that all bound ligand was removed. Unliganded β_2AR365 was then eluted with buffer F plus Flag peptide (100 μg ml^{-1}). Glycosylations were removed by treatment with PNGase F as described earlier. Receptor was dialysed against buffer A with a 20-kDa cutoff dialysis cassette (Slide-A-Lyzer; Pierce) to ensure the removal of Flag peptide before [^{13}C]methylation. Flag peptide (amino-acid sequence DYKDDDDK) has three primary amines that can be [^{13}C]methylated and cause undesirable NMR background.

Unliganded β_2AR365 was reductively methylated (as described earlier), dialysed against buffer A to remove labelling reagents, dialysed against buffer A prepared in 98% ^2H_2O, and concentrated for NMR as described above. This method was used to prepare the samples shown in Figs 3 and 4 and Supplementary Figs 12 and 15. Ligand additions to unliganded [^{13}C]methyl-365N NMR samples were made from ligand stocks dissolved in perdeuterated dimethyl d_6-sulfoxide (DLM-10-10; Cambridge Isotope Labs). (*R*,*R*)-formoterol was a gift from Sepracor.

Preparation of carazolol-bound [^{13}C]methyl-β_2AR365 mutants for Lys 305 peak assignment. To facilitate the assignment of dimethyllysine peaks 1 and 2 (Fig. 2a), we developed a small-scale expression and purification technique that yields an NMR sample of carazolol-bound β_2AR365 (about 2–3 mg) from 1–2 litres of Sf9 cells. We modified β_2AR365 to include a carboxy-terminal hexahistidine tag for nickel affinity chromatography[31]. Six histidine codons were added to the β_2AR365 cDNA between the Gly 365 and STOP codons (β_2AR365-His).

To maximize the yield of β_2AR365-His, we added 200 nM carazolol directly to the culture medium at the time of infection with baculovirus. Buffers for all subsequent purification steps also included a minimum of 200 nM carazolol. We have observed that inverse agonists improve cell-surface expression and help to stabilize the receptor during solubilization. However, the affinity of β_2AR for carazolol ($K_d < 0.1$ nM) is sufficiently high for binding to be essentially irreversible. This precludes the use of alprenolol-Sepharose chromatography as a functional purification step. Instead, β_2AR365-His was first purified by Flag affinity chromatography. Reactive cysteine residues were alkylated as described above, and the protein was dialysed extensively against buffer A to remove Flag peptide. Reductive methylation was performed as described above. [^{13}C]Methyl-β_2AR365-His was then purified by nickel affinity chromatography (Chelating Sepharose Fast Flow; GE Healthcare) as described previously[31]. Final NMR dialysis and concentration were performed as described above. This method was used to prepare the samples shown in Fig. 2b, c and Supplementary Figs 10 and 11.

Crystallographic data collection and processing. Crystals of reductively methylated β_2AR365–Fab5 complex were generated essentially as described in ref. 3 and were isomorphous to the non-methylated receptor–Fab5 complex. Data collection was performed with the 10-μm collimated microfocus beamline 23ID-B of the Advanced Photon Source at Argonne National Laboratory. A data set comprising 316° of oscillation data was obtained from a single crystal (see Supplementary Table 2). Because of radiation damage, only 5–10° of data (1° per frame) could be measured before the crystal was translated to a new position. Data were processed with HKL2000 (ref. 35). Similarly to the previous β_2AR24/365–Fab5 complex data reduction, global post-refinement of the unit-cell parameters was not performed. Rather, the unit-cell parameters were obtained from indexing and refinement from one wedge of data, and were subsequently used for processing the remaining data without unit-cell constant refinement.

Structure solution and refinement. The structure of the methylated β_2AR365–Fab5 complex was solved by initially performing rigid-body refinement in CNS[36] using the unmethylated β_2AR24/365–Fab5 complex structure (PDB accession code 2R4S) as a single rigid body. This gave *R* and R_{free} values of 0.358 and 0.348, respectively. Multiple rounds of manual rebuilding, positional refinement, grouped temperature factor refinement and Translation–Libration–Screw (TLS) refinement were performed with the PHENIX package[37], bringing *R* and R_{free} values down to 0.233 and 0.274, respectively. As in the previous β_2AR24/365–Fab5 complex refinement[3], only those residues that could be unambiguously assigned were included in the final model. In addition to the residues present in the β_2AR24/365–Fab5 structure (PDB accession code 2R4S), receptor residues 35–36, 91 and 307–310 were included in the methylated β_2AR365–Fab5 model. The following receptor residues were modelled as alanine because of insufficient electron density to model full side chains: 36, 39, 42, 49, 53, 55, 63, 69, 77, 112, 114, 120, 122, 131, 147, 156, 209, 227, 232, 263, 279, 287, 308, 309, 321, 324, 326 and 332.

31. Kobilka, B. K. Amino and carboxyl terminal modifications to facilitate the production and purification of a G protein-coupled receptor. *Anal. Biochem.* **231**, 269–271 (1995).

32. Yao, X. J. *et al.* The effect of ligand efficacy on the formation and stability of a GPCR–G protein complex. *Proc. Natl Acad. Sci. USA* **106,** 9501–9506 (2009).
33. Tota, M. R. & Strader, C. D. Characterization of the binding domain of the β-adrenergic receptor with the fluorescent antagonist carazolol. Evidence for a buried ligand binding site. *J. Biol. Chem.* **265,** 16891–16897 (1990).
34. Baker, J. G. The selectivity of β-adrenoceptor antagonists at the human β_1, β_2 and β_3 adrenoceptors. *Br. J. Pharmacol.* **144,** 317–322 (2005).
35. Otwinowski, Z. & Minor, W. Processing of X-ray diffraction data collected in oscillation mode. *Macromol. Crystallogr. A* **276,** 307–326 (1997).
36. Brunger, A. T. *et al.* Crystallography & NMR system: a new software suite for macromolecular structure determination. *Acta Crystallogr. D* **54,** 905–921 (1998).
37. Adams, P. D. *et al.* PHENIX: building new software for automated crystallographic structure determination. *Acta Crystallogr. D* **58,** 1948–1954 (2002).